

Does Nature Click? Theoretical Prediction of an Enzyme-Catalyzed Transannular 1,3-Dipolar Cycloaddition in the Biosynthesis of Lycojaponicumins A and B

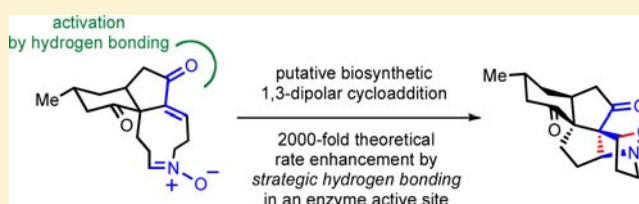
Elizabeth H. Krenske,^{*,†} Ashay Patel,[‡] and K. N. Houk^{*,‡}

[†]School of Chemistry and Molecular Biosciences, University of Queensland, Brisbane, Queensland 4072, Australia

[‡]Department of Chemistry and Biochemistry, University of California, Los Angeles, California 90095, United States

S Supporting Information

ABSTRACT: Biosynthetic 1,3-dipolar cycloadditions are rare. No enzymes have yet been identified whose function is to catalyze this class of reactions. Recently, however, a 1,3-dipolar cycloaddition was proposed as a key step in the biosynthesis of two *Lycopodium* alkaloids, lycojaponicumins A and B. The lycojaponicumins' fused bicyclic tetrahydroisoxazole ring system was proposed to originate from a transannular 1,3-dipolar cycloaddition between a nitron and an enone in a nine-membered macrocycle. We have used quantum mechanical calculations to predict whether this cycloaddition could constitute a feasible step in a biosynthetic pathway. Our calculations define a general computational approach for analyzing whether a putative biosynthetic reaction is likely to be enzyme-catalyzed. The quantum mechanically predicted rate of the uncatalyzed reaction in water is compared with the rate enhancement theoretically achievable when the reaction is catalyzed by a theozyme (theoretical enzyme). Density functional theory calculations (M06-2X) predict that the uncatalyzed transannular 1,3-dipolar cycloaddition of the putative lycojaponicumins precursor in water is moderately facile ($\Delta G^\ddagger = 21.5$ kcal/mol, $k = 10^{-3}$ s⁻¹) and that an enzyme could accelerate the cycloaddition by placing hydrogen bond donors around the enone while maintaining an otherwise nonpolar active site. The theoretical enzyme-catalyzed process has $\Delta G^\ddagger \approx 17$ kcal/mol, corresponding to a 2000-fold rate enhancement, and the predicted k_{cat} (2 s⁻¹) is similar to those of known enzymes involved in secondary metabolic pathways. Thus, theory predicts that the proposed transannular 1,3-dipolar cycloaddition is a plausible step in a biosynthetic pathway leading to the lycojaponicumins and suggests that dipolar cycloadditions can be accelerated by enzyme catalysis.



INTRODUCTION

The 1,3-dipolar cycloaddition is one of the most efficient ways to synthesize heterocycles. Many 1,3-dipolar cycloadditions (including the classic azide–alkyne coupling) have been classified as “click reactions”: clean, high-yielding reactions that assemble products with well-defined stereochemistry from simple precursors in a modular fashion that mimics nature.¹ Considering the utility of click dipolar cycloadditions in organic synthesis, the dearth of 1,3-dipolar cycloadditions in nature is perplexing. Only a handful of natural products have been identified that can be speculatively traced to 1,3-dipolar cycloadditions (involving nitrones,^{2–4} oxidopyrylium ions,^{5–7} or azomethine ylides⁸), and little is known about how these reactions might be facilitated in vivo. The scarcity of biological 1,3-dipolar cycloadditions contrasts dramatically with the growing number of known biosynthetic Diels–Alder reactions.^{9–11}

Recently, Yu and co-workers proposed¹² an intriguing biosynthetic mechanism, featuring a 1,3-dipolar cycloaddition, for the newly discovered alkaloids, lycojaponicumins A and B (Scheme 1). The lycojaponicumins were isolated from the club moss *Lycopodium japonicum* and are surmised to derive from fawcettimine. Yu et al. suggested that the unusual bicyclic

tetrahydroisoxazole framework of the lycojaponicumins is formed by the transannular nitron–enone 1,3-dipolar cycloaddition **1** → **2**. While the details of the lycojaponicumins biosynthetic pathway still await elucidation, Yu's proposed mechanism represents an intriguing new lead in the search for the first authentic¹³ 1,3-dipolar cycloaddition-ase. Prompted by the potential significance of such an enzyme's existence, we have used quantum mechanical calculations to investigate the feasibility of the proposed biosynthetic 1,3-dipolar cycloaddition of **1**. Our calculations, reported here, represent a general computational approach for analyzing whether a given biosynthetic reaction is likely to require enzymatic catalysis.

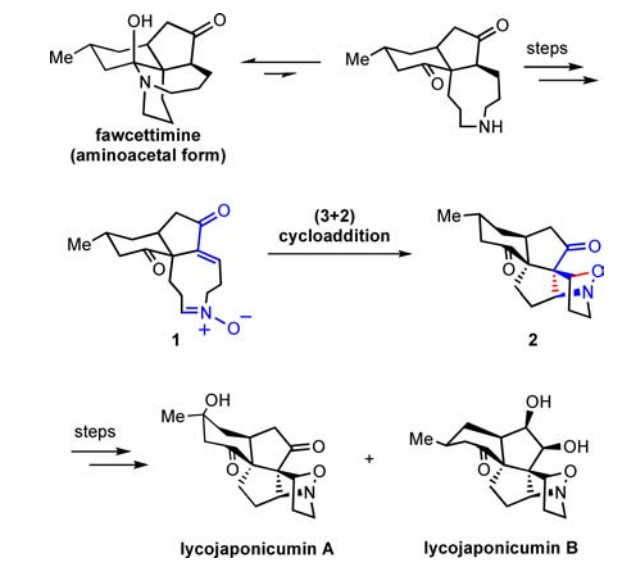
RESULTS AND DISCUSSION

The first stage of our investigation involved prediction of the rate constant for the uncatalyzed transannular 1,3-dipolar cycloaddition **1** → **2**. Computations began with conformational searches of the reactant and transition state at the M06-2X/6-31+G(d,p) level, followed by single-point energy calculations on the important conformers at the M06-2X/def2-TZVPP

Received: September 25, 2013

Published: November 6, 2013

Scheme 1. Proposed Biosynthetic 1,3-Dipolar Cycloaddition Pathway Leading to Lycojaponicumins A and B, As Suggested by Yu and Co-workers¹²



level. The results of the gas-phase calculations are shown in Figure 1. Macroyclic nitronone **1** was found to have four low energy conformers (**1a–d**), the most stable of which is **1a**. In three conformers (**1a–c**), the nine-membered ring adopts a tublike geometry, with the nitronone moiety poised below the enone C=C bond. These conformers are connected to the cycloaddition transition states **TS1a–c**, respectively. The fourth reactant conformer (**1d**) contains a chairlike nine-membered ring. This conformer is not directly connected to a TS, since the nine-membered ring must adopt the tub conformation before the cycloaddition can take place. The chair conformer is 1.1 kcal/mol higher in energy than the tub (ΔG). Among the transition states, **TS1a** is lowest in energy in the gas phase, with an activation energy (ΔG^\ddagger) of 21.2 kcal/mol; **TS1c** is 1 kcal/mol higher in energy, and **TS1b** is 3.2 kcal/mol higher in energy (than **TS1a**).

To estimate the activation energy of the uncatalyzed cycloaddition in water, we reoptimized the reactant and TS in implicit solvent (IEFPCM), both in the absence and presence of additional explicit water molecules (Figure 2).¹⁴ Carbonyl groups are well-known to accept two strong hydrogen bonds through the oxygen lone pairs;¹⁵ calculations on a nitronone–alkene 1,3-dipolar transition state indicate that the nitronone oxygen likewise accepts two hydrogen bonds. Thus, the microsolvated transition state **TS4** was constructed with four explicit water molecules satisfying the hydrogen bonds around the nitronone and enone.¹⁶

Optimization of the transition states in implicit solvent (**TS1a'**, **TS1c'**) has only a minor effect on the transition state geometries, but does affect the relative stabilities of the transition states, such that **TS1c'** is lowest in energy, 1.7 kcal/mol lower than **TS1a'**. The “c” transition-state conformer has a larger dipole moment than the “a” conformer (11.7 D for **TS1c'**, cf. 6.9 D for **TS1a'**) and as a result benefits from a greater free energy of solvation, explaining why **TS1c'** is more stable than **TS1a'** in water. The most stable reactant conformation in solution remains the “a” conformer. The reaction will proceed primarily via the “c” transition state provided that reactants a and c are in rapid equilibrium (via

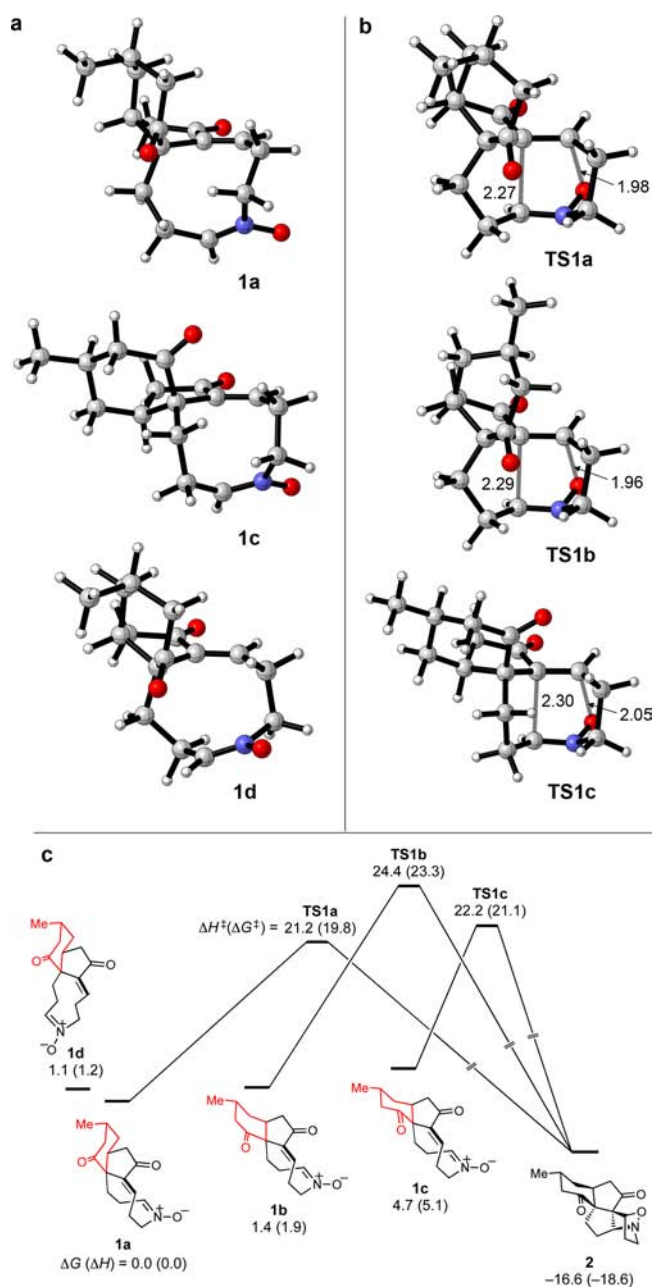


Figure 1. Transannular nitronone–enone 1,3-dipolar cycloaddition of the putative lycojaponicumins precursor **1** in the gas phase. (a) Selected reactant geometries. (b) Transition state geometries. (c) Free energy profiles for the transannular 1,3-dipolar cycloaddition in the gas phase. Free energies (with enthalpies in parentheses) are reported at the M06-2X/def2-TZVPP//M06-2X/6-31+G(d,p) level of theory (kcal/mol).

chair–chair interconversion of the cyclohexanone ring). Coordination of two water molecules simultaneously to the nitronone and the enone (**TS2**) appears destabilizing, raising ΔG^\ddagger by about 1 kcal/mol, but coordination of two water molecules to the enone alone (**TS3**) lowers ΔG^\ddagger by up to 3.7 kcal/mol. Transition state **TS4**, which is the most accurate model for the uncatalyzed cycloaddition in water, has $\Delta G^\ddagger = 21.5$ kcal/mol, similar to the corresponding transition state with no explicit waters (**TS1c'**). This value of ΔG^\ddagger corresponds to a rate constant of $1 \times 10^{-3} \text{ s}^{-1}$ and a half-life of approximately 10 min at room temperature.

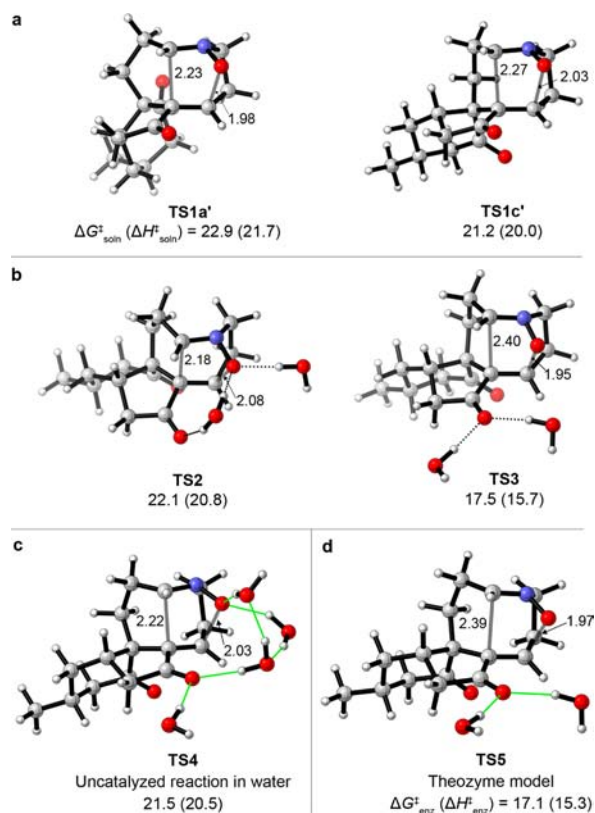


Figure 2. Prediction of the rate of the uncatalyzed transannular 1,3-dipolar cycloaddition of **1** and the theoretical enzymatic rate acceleration. (a) Transition states for the transannular 1,3-dipolar cycloaddition of **1** optimized in implicit water without any additional explicit water molecules. (b) Partially microsolvated transition states modeling the effect of hydrogen bonding to the nitrone and/or enone. (c) Transition state in which all hydrogen bonds around the nitrone and enone oxygens are satisfied, modeling the uncatalyzed reaction in water. (d) Theozyme model comprising strategic hydrogen bonding to the enone within a nonpolar active site. All transition states except for **TS5** were optimized in implicit water (IEFPCM) at the M06-2X/6-31+G(d,p) level. **TS5** was optimized in implicit diethyl ether in order to simulate the dielectric constant of the interior of an enzyme. Subsequent single-point calculations at the M06-2X/def2-TZVPP level, in conjunction with the solution-optimized geometries, gave the activation free energies (and enthalpies in parentheses) shown (kcal/mol). The activation energies for **TS2**–**TS5** are computed relative to the nearest conformer of the reactant complex, while the activation energies for **TS1a'** and **TS1c'** are computed relative to the most stable conformer of the reactant.

Theory therefore predicts that the uncatalyzed transannular 1,3-dipolar cycloaddition of **1** in water is moderately facile. The nitrone **1**, being a dialkyl-substituted nitrone, is potentially quite susceptible to hydrolysis,¹⁷ but the macrocyclic structure may be expected to suppress any hydrolytic degradation of substrate. In principle, an enzyme could accelerate the cycloaddition of **1** if it could capitalize on the stabilization that can be derived from selective hydrogen bonding to the enone (cf. **TS3**). The rate enhancement available through hydrogen bonding to the enone within a typical dielectric environment of an enzyme active site was modeled by reoptimizing **TS3** in implicit diethyl ether ($\epsilon = 4.24$). The ether-optimized transition state is labeled **TS5** in Figure 3. **TS5** represents a theozyme^{18,19} for the cycloaddition of **1**: the two water molecules mimic the role that hydrogen bond donors

such as Ser, Thr, or Tyr could play in an actual enzyme. The theozyme-catalyzed cycloaddition of **1** has a predicted ΔG^\ddagger of 17.1 kcal/mol. This value is 4.4 kcal/mol lower than that of the uncatalyzed reaction and corresponds to a k_{cat} of about 2 s^{-1} . Thus, the theozyme calculation suggests that by placing hydrogen-bond donors strategically around the enone, an enzyme could provide a rate enhancement of about 2000-fold, allowing the cycloaddition of **1** to proceed with a half-life of about 0.4 s at 25 °C.

Even in the absence of an enzyme catalyst, the proposed cycloaddition of **1** appears to be a rather low energy process. In comparison, the known intramolecular (but not transannular) 1,3-dipolar cycloadditions of C-alkenyl nitrones **6** (Scheme 2a) are reported^{20,21} to occur over periods of hours to days at temperatures between 0 °C and room temperature in Et₂O or CH₂Cl₂. These reactions, studied by Aurich, lead to 5,5-bicyclic ring systems related to the 5,5,5-tricyclic ring system of the lycojaponicumins. Comparable intermolecular nitrone–alkene 1,3-dipolar cycloadditions are much more sluggish: for example, the cycloaddition of *N*-benzyl *C*-ethyl nitrone with ethyl crotonate (Scheme 2b) was reported by Huisgen²² to have a rate constant on the order of $10^{-4} \text{ L mol}^{-1} \text{ s}^{-1}$ at 100 °C in toluene.

The factors leading to high reactivity in the cyclic substrate **1** were analyzed by examination of a series of nitrone cycloadditions involving the model substrates shown in Figure 3. Starting with the reference intermolecular cycloaddition of the parent nitrone with *cis*-butene (**TS6**), models of increasing complexity were built up by incorporating, one at a time, the structural features of tricyclic reactant **1**. The intermolecular reference reaction has a ΔG^\ddagger (30.3 kcal/mol) 9 kcal/mol higher than the proposed biogenetic dipolar cycloaddition. The majority of this difference (6 kcal/mol) is captured in the first step of the series (**TS6** → **TS7**) and is the result of incorporating the cycloaddends into the nine-membered ring. The transannular transition state **TS7** has an activation enthalpy (ΔH^\ddagger) that is 8.5 kcal/mol higher than that of the intermolecular **TS6**, but it has a tiny entropic term ($-T\Delta S^\ddagger = 1.7 \text{ kcal/mol}$), which is 14.3 kcal/mol smaller than the $-T\Delta S^\ddagger$ of the intermolecular reaction **TS6** and makes ΔG^\ddagger overall smaller by 5.8 kcal/mol. This entropy compensation in **TS7** exceeds the typical effect of intramolecularity by a few kcal/mol. Next, the fusion of the nine-membered ring into a tricyclic system (**TS7** → **TS8**) lowers ΔG^\ddagger by 1.4 kcal/mol. This decrease is mostly enthalpic and arises because the tricyclic ring system predisposes the nine-membered ring to adopt a more reactive conformation. As shown in the inset to Figure 3, the parent nine-membered cyclic nitrone **7** prefers to adopt a chairlike structure rather than the tub. In **1**, on the other hand, the chair (**1d**, Figure 1) is destabilized by electrostatic repulsion between the nitrone and the cyclohexanone carbonyl group. The absence of a low-lying chair form in **1** preorganizes this reactant into a conformation closer to the transition state, reducing the barrier to cycloaddition by about 1 kcal/mol. Finally, a further 2 kcal/mol of activation is derived from the α -carbonyl substituent on the dipolarophile (**TS8** → **TS1a**).

CONCLUSION

Does nature click? Although the definitive answer to this question will only come from experiment, our assessment of the rate of the purported 1,3-dipolar cycloaddition of **1** suggests an affirmative answer. Density functional theory calculations

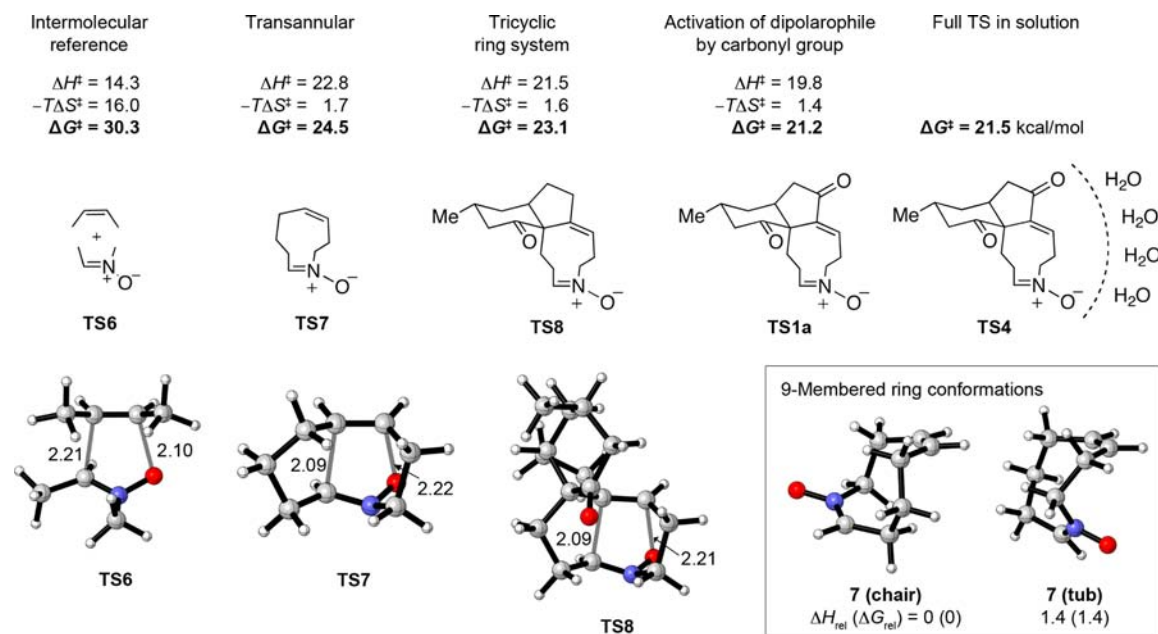
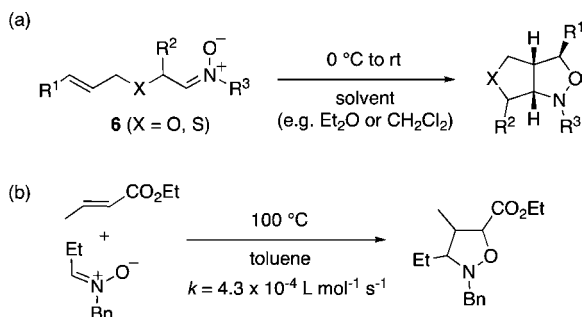


Figure 3. Analysis of the factors giving rise to the low barrier for transannular cycloaddition of **1**.

Scheme 2. Related Intra- and Intermolecular Nitrono Cycloadditions: (a) Facile Intramolecular Nitrono–Alkene Cycloadditions;^{20,21} (b) Sluggish Intermolecular Nitrono–Alkene Cycloaddition²²



predict a k_{uncat} of about 10^{-3} s^{-1} for the uncatalyzed 1,3-dipolar cycloaddition of the putative lycojaponicum precursor **1**, suggesting that the reaction might even occur without the assistance of an enzyme. The predicted k_{cat} for the enzyme-catalyzed cycloaddition of **1**, based on a theozyme model where the TS is stabilized by coordination of two hydrogen-bond donors to the enone, is about 2 s^{-1} . The predicted k_{cat} is small compared to the catalytic constants of the most efficient known enzymes, which are on the order of 10^3 – 10^7 s^{-1} .²³ However, such large catalytic constants are generally only observed for highly evolved enzymes that are involved in primary metabolism. Enzymes that are involved in secondary metabolic pathways commonly display much smaller k_{cat} values on the order of 0.01 – 1 s^{-1} .²⁴ The predicted k_{cat} for the reaction **1** \rightarrow **2** falls within this range. Thus, theory predicts that the reaction could be spontaneous, but enzyme catalysis will be necessary to bring the reaction rate into the realm generally occupied by enzyme-catalyzed reactions involved in secondary metabolism.

THEORETICAL CALCULATIONS

Quantum Mechanical Calculations. All quantum mechanical calculations were performed using Gaussian 09.²⁵ Geometry optimizations were conducted with the hybrid meta-GGA density

functional M06-2X²⁶ and the 6-31+G(d,p) basis set. Normal mode analysis was used to confirm that optimized reactants and products were indeed minima and that transition states were first-order saddle points. Geometry optimizations were followed by M06-2X single-point calculations using the triple- ζ def2-TZVPP^{27,28} basis set. The enthalpies and free energies reported (at 25 °C) were determined by adding the thermal and zero-point corrections determined at the M06-2X/6-31+G(d,p) level of theory to the M06-2X/def2-TZVPP single point energies. A standard state of 1 mol L^{-1} is used. Errors in computed entropies, introduced by the treatment of low frequency modes as harmonic motions, were minimized by use of Truhlar's approximation,²⁹ in which all harmonic frequencies below 100 cm^{-1} were raised to exactly 100 cm^{-1} before evaluation of the vibrational component of the thermal contribution to entropy. Several stationary points were also optimized in implicit solvent (water or diethyl ether) using the IEFPCM solvation model.³⁰ Subsequent M06-2X/def2-TZVPP (gas-phase) single-point calculations were used in conjunction with the IEFPCM solvation energy and vibrational corrections to compute the solution-phase activation barriers. The “ultrafine” numerical integration grid of Gaussian 09, consisting of 99 radial shells and 590 angular points per shell, was used throughout.

Conformational Analysis. Conformational analyses of the reacting macrocycles **1** and **7** were performed using the MMFF force field in MacroModel 9.9.³¹ We utilized a newly implemented search methodology that incorporates short molecular dynamics simulations into a low mode/Monte Carlo search protocol optimized for the conformational sampling of macrocycles. A total of 5000 simulation cycles and 5000 Monte Carlo steps were performed, using the GB/SA model to simulate solvation in water. For **1**, the search yielded 15 distinct low energy conformers within 10 kcal/mol of the lowest MMFF energy, while for **7** seven conformers were found. The global minimum among each set of conformers was identified after M06-2X/6-31+G(d,p) reoptimizations of the MMFF structures.

ASSOCIATED CONTENT

Supporting Information

Computational data and a complete citation for ref 25. This material is available free of charge via the Internet at <http://pubs.acs.org>.

AUTHOR INFORMATION

Corresponding Authors

e.krenske@uq.edu.au

houk@chem.ucla.edu

Notes

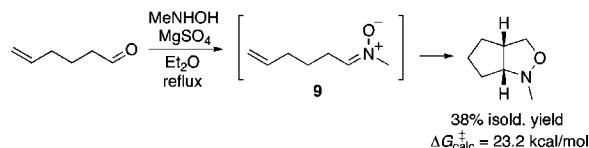
The authors declare no competing financial interest.

ACKNOWLEDGMENTS

We acknowledge the financial support of the Australian Research Council (FT120100632 to E.H.K.) and the NSF (CHE-1059084 to K.N.H.). A.P. thanks the Chemistry–Biology Interface program (T32 GM 008496) for its support. High-performance computing resources were provided by the Australian National Computational Infrastructure National Facility, the University of Queensland Research Computing Centre, the UCLA Hoffman2 cluster, and the NSF Extreme Science and Engineering Discovery Environment (TG-CHE040013N). We are grateful to Evan Styduhar and Professor Yi Tang for helpful discussions.

REFERENCES

- Kolb, H. C.; Finn, M. G.; Sharpless, K. B. *Angew. Chem., Int. Ed.* **2001**, *40*, 2004–2021.
- Rao Irlapati, N.; Baldwin, J. E.; Adlington, R. M.; Pritchard, G. J.; Cowley, A. R. *Tetrahedron* **2005**, *61*, 1773–1784.
- Zhao, B.-X.; Wang, Y.; Zhang, D.-M.; Jiang, R.-W.; Wang, G.-C.; Shi, J.-M.; Huang, X.-J.; Chen, W.-M.; Che, C.-T.; Ye, W.-C. *Org. Lett.* **2011**, *13*, 3888–3891.
- Zhao, B.-X.; Wang, Y.; Zhang, D.-M.; Huang, X.-J.; Bai, L.-L.; Yan, Y.; Chen, J.-M.; Lu, T.-B.; Wang, Y.-T.; Zhang, Q.-W.; Ye, W.-C. *Org. Lett.* **2012**, *14*, 3096–3099.
- Tang, B.; Bray, C. D.; Pattenden, G. *Org. Biomol. Chem.* **2009**, *7*, 4448–4457.
- Sugano, Y.; Kikuchi, F.; Toita, A.; Nakamura, S.; Hashimoto, S. *Chem.—Eur. J.* **2012**, *18*, 9682–9690.
- Wang, S. C.; Tantillo, D. J. *J. Org. Chem.* **2008**, *73*, 1516–1523.
- Borowski, T.; de Marothy, S.; Broclawik, E.; Schofield, C. J.; Siegbahn, P. E. M. *Biochemistry* **2007**, *46*, 3682–3691.
- Stocking, E. M.; Williams, R. M. *Angew. Chem., Int. Ed.* **2003**, *42*, 3078–3115.
- Oikawa, H. *Bull. Chem. Soc. Jpn.* **2005**, *78*, 537–554.
- Campbell, C. D.; Vederas, J. C. *Biopolymers* **2010**, *93*, 755–763.
- Wang, X.-J.; Zhang, G.-J.; Zhuang, P.-Y.; Zhang, Y.; Yu, S.-S.; Bao, X.-Q.; Zhang, D.; Yuan, Y.-H.; Chen, N.-H.; Ma, S.-g.; Qu, J.; Li, Y. *Org. Lett.* **2012**, *14*, 2614–2617.
- Finn, Sharpless, and co-workers reported that 1,2,3-triazole-containing inhibitors of acetylcholinesterase could be selectively synthesized from a parallel array of azide and alkyne building blocks by 1,3-dipolar cycloaddition in the presence of acetylcholinesterase. In this case, the enzyme is not an authentic 1,3-dipolar cycloadditionase but instead accelerates a non-natural 1,3-dipolar cycloaddition. See: Lewis, W. G.; Green, L. G.; Grynszpan, F.; Radić, Z.; Carlier, P. R.; Taylor, P.; Finn, M. G.; Sharpless, K. B. *Angew. Chem., Int. Ed.* **2002**, *41*, 1053–1057.
- Huisgen (ref 22) reported rate constants for intermolecular 1,3-dipolar cycloadditions of C-phenyl N-methylnitronone with various alkenes, mostly in nonpolar solvents. M06-2X calculations (see the Supporting Information) on representative cycloadditions of this nitronone with methyl acrylate, ethyl crotonate, maleic anhydride, and dimethyl acetylenedicarboxylate were found to overestimate ΔG^\ddagger , presumably because of difficulties in accurately computing entropies of activation in solution, but much better accuracy is obtained for intramolecular nitronone–alkene cycloadditions. For example, LeBel et al. reported that the intramolecular cycloaddition of C-alkenylnitronone **9** gave a 38% isolated yield of cycloadduct over eight hours in refluxing Et₂O, while Aurich's cycloadditions of alkenylnitronones **6** (Scheme 2a), which furnish related 5,5-bicyclic ring systems, occur over periods of hours to days at temperatures between 0° C and room temperature (refs 20 and 21). M06-2X calculations on the cycloaddition of **9** predict a ΔG^\ddagger of 23.2 kcal/mol ($t_{1/2} \approx 50$ min) in refluxing Et₂O, in good agreement with experiment. The experimental study of the cycloaddition of **9** is reported in: LeBel, N. A.; Post, M. E.; Whang, J. J. *J. Am. Chem. Soc.* **1964**, *86*, 3759–3767.



(15) *Hydrogen Bonding in Organic Synthesis*; Pihko, P. M., Ed.; Wiley-VCH: Weinheim, 2009.

(16) The most stabilizing hydrogen-bonding arrangement for two water molecules around a carbonyl group is a planar arrangement. However, based on an analysis of enzyme crystal structures, Simón and Goodman have shown that the most common hydrogen-bonding geometry in oxyanion holes is a “grand jeté” arrangement, where the hydrogen bond donors are positioned approximately perpendicular to the carbonyl plane. Simón and Goodman showed that an in-plane arrangement of hydrogen bond donors stabilizes an oxyanion-like transition state more than a grand jeté arrangement, but the stabilization of the corresponding reactant by in-plane hydrogen bonding is even greater; thus, overall less stabilization is lost on going from reactant to TS in the grand jeté arrangement, explaining why the grand jeté arrangement is effective for catalysis. See: (a) Simón, L.; Goodman, J. M. *J. Org. Chem.* **2010**, *75*, 1831–1840. (b) Simón, L.; Goodman, J. M. *Org. Biomol. Chem.* **2012**, *10*, 1905–1913.

(17) Hamer, J.; Macaluso, A. *Chem. Rev.* **1964**, *64*, 473–495.

(18) Tantillo, D. J.; Chen, J.; Houk, K. N. *Curr. Opin. Chem. Biol.* **1998**, *2*, 743–750.

(19) Tantillo, D. J.; Houk, K. N. In *Stimulating Concepts in Chemistry*; Vögtle, F., Stoddart, J. F., Shibasaki, M., Eds.; Wiley-VCH: Weinheim, 2005.

(20) Aurich, H. G.; Ruiz Quintero, J.-L. *Tetrahedron* **1994**, *50*, 3929–3942.

(21) Baskaran, S.; Aurich, H. G.; Biesemeier, F.; Harms, K. *J. Chem. Soc., Perkin Trans. 1* **1998**, 3717–3724.

(22) Huisgen, R.; Seidl, H.; Brüning, I. *Chem. Ber.* **1969**, *102*, 1102–1116.

(23) Fersht, A. *Structure and Mechanism in Protein Science*; W. H. Freeman: New York, 1999; Chapter 4.

(24) Two recent examples of catalytic constants for enzymes involved in secondary metabolism include a k_{cat} of 48.4 min⁻¹ for acyl transfer from α -S-methylbutyryl-LovF to monacolin J catalyzed by LovD and a k_{cat} of 1.42 min⁻¹ for a geranyl transfer reaction catalyzed by VrtC. See: (a) Xie, X.; Meehan, M. J.; Xu, W.; Dorrestein, P. C.; Tang, Y. *J. Am. Chem. Soc.* **2009**, *131*, 8388–8389. (b) Chooi, Y.-H.; Wang, P.; Fang, J.; Li, Y.; Wu, K.; Wang, P.; Tang, Y. *J. Am. Chem. Soc.* **2012**, *134*, 9428–9437.

(25) Frisch, M. J., et al. Gaussian 09, Revision C.01, Gaussian, Inc., Wallingford, CT, 2010.

(26) Zhao, Y.; Truhlar, D. G. *Theor. Chem. Acc.* **2008**, *120*, 215–241.

(27) Weigend, F.; Ahlrichs, R. *Phys. Chem. Chem. Phys.* **2005**, *7*, 3297–3305.

(28) Schäfer, A.; Huber, C.; Ahlrichs, R. *J. Chem. Phys.* **1994**, *100*, 5829–5835.

(29) Zhao, Y.; Truhlar, D. G. *Phys. Chem. Chem. Phys.* **2008**, *10*, 2813–2818.

(30) See, for example: Tomasi, J.; Mennucci, B.; Cammi, R. *Chem. Rev.* **2005**, *105*, 2999–3093 and references cited therein.

(31) MacroModel, version 9.9, Schrödinger, LLC, New York, NY, 2012.